Egypt. J. Chem. **Vol. 68**, No. 5 pp. 23 - 35 (2025)

Egyptian Journal of Chemistry

http://ejchem.journals.ekb.eg/

Discovery of Novel Natural Compounds for Inhibiting JNK Signaling in Cancer: Multi-Step Virtual Screening, MM-GBSA Calculations, and Molecular Dynamics Simulations

Abdulrahim A. Alzain,[1,*] Rayan Yousif,[1] Mohammed A. Almogaddam,[1] Hazem G. A. Hussein,[2]Ehda Ahmad Awad,[3] Ahmed Mohammad Alraddadi,[3] Shaimaa G. A. Mohamed, [4] Abdullah L. Alalawi,[5] Gamal A. Mohamed,[6] Abdulmajeed M. Althubyani,[7] Sabrin R. M. Ibrahim [8,9,*]

[1] *Department of PharmaceuticalChemistry, Faculty of Pharmacy, University of Gezira, Gezira, Sudan*

[2] *Preparatory Year Program, Batterjee Medical College, Jeddah 21442, Saudi Arabia*

[3] *Prince Mohammed Bin Abdulaziz Hospital-Al Madinah Al Munawarah-NGHA, Ministry of National Guard Health Affairs, Al Madinah Al Munawarah 41511, Saudi Arabia*

[4] *Faculty of Dentistry, British University, El Sherouk City, Suez Desert Road, Cairo 11837, Egypt*

[5] *Pharmaceutical Care Services, King Salman Medical City, MOH, Al Madinah Al Munawwarah 11176, Saudi Arabia*

[6] *Department of Natural Products and Alternative Medicine, Faculty of Pharmacy, King Abdulaziz University, Jeddah 21589, Saudi Arabia*

[7] *Anesthesia Department, King Fahad hospital, MOH, Al Madinah Al Munawwarah, Saudi Arabia*

[8] *Preparatory Year Program, Department of Chemistry, Batterjee Medical College, Jeddah 21442, Saudi Arabia*

[9] *Department of Pharmacognosy, Faculty of Pharmacy, Assiut University, Assiut 71526, Egypt*

Abstract

Human c-Jun N-terminal kinase 1 (JNK1) is a cytosolic kinase within the mitogen-activated protein kinasefamily, pivotal in intracellular signal transduction cascades. Overexpression of JNK1 implicated in various cancers. Despite some JNK1 inhibitors progressing to clinical trials, none have gained market approval, underscoring the urgent need for new candidates. Computer-aided drug design lowers the expenses and time required for drug development. Rough estimates indicate that computational processes take less than one-third of the usual time and cost. This research employs diverse *in silico* screening methods to rapidly identify inhibitors for JNK1 associated with cancer. Specifically, we employed pharmacophore modeling on the bound ligand of JNK1 protein to identify essential pharmacophoric features crucial for discovering potential inhibitors. These features were screened against 449,008 natural compounds sourced from the SN3 database. The identified compounds underwent docking and MM-GBSA calculations. Two compounds (SN0239242 and SN0263268) exhibited superior MM-GBSA binding affinity compared to the bound ligand, with values of -69.22, -62.2, and -57.68 kcal/mol, respectively. These compounds were subjected to 100 ns molecular dynamics experiments and exhibited stable interactions. Natural compounds from these *in silico* studies showed promising anticancer potential as JNK1 inhibitors and could be prioritized for future experimental validation.

Keywords: Cancer; JNK1; Natural compounds; Docking; Molecular Dynamics; Health and wellbeing; Drug discovery

1. Introduction

Mitogen-activated protein kinases (MAPKs) constitute a crucial family within protein kinases, playing a pervasive role in various cellular regulatory mechanisms and activities. Three key signaling cascade enzymes drive the activity, regulatory functions of MAPKs, andorchestrate signaling events through the phosphorylation of targeted proteins from the cell surface to the nucleus. These enzymes include extracellular signal-regulated kinases (ERKs), c-Jun amino terminal kinases (JNKs), and p38 MAPKs [1,2].

JNKs activate a principal component of the AP-1 heterodimer transcription factor, the C-Jun proto-oncogene, through phosphorylation of its serine 63 and 73 residues. Other transcription factors affected by JNKs include ELK1, activating transcription factor 2 (ATF-2), signal transducers and activators of transcription (STAT3), nuclear factor of activated T-cells 4 (NFAT4), tumor protein p53 (p53), and Smad4. JNKs are also referred to as stress-activated protein kinases (SAPKs) [3–5].

The molecular cloning of human JNK protein kinases in 1996 revealed ten different isoforms derived from three gene types: JNK1 (Mapk8), JNK2 (Mapk9), and JNK3 (Mapk10) [6–8]. These JNK protein kinases play a pivotal role in various cellular responses, including cellular proliferation, apoptosis, gene expression, oncogenic transduction, migration, and inflammation, primarily mediated through their impact on the AP-1 transcriptional factor. The activation of JNK protein kinase pathways involves diverse molecules, such as extracellular stimuli activators, GTP-binding small proteins, MAPKKs and MAPKKKs,

*Corresponding author e-mail: sabrin.ibrahim@bmc.edu.sa.; (Sabrin R. M. Ibrahim).

Received date 14 June 2024; Revised date 07 September 2024; Accepted date 10 September 2024

DOI: 10.21608/EJCHEM.2024.297681.9866

ST20 homologous and related proteins, phosphoinositide-3-kinase, and other activators as outlined in studies by Minden and Karin [9–12].

JNK-1 proteins can be activated by stress stimuli, including UV irradiation and the introduction of proteins from oncogenes. This activation can enhance cancer cell production through mechanisms like uncontrolled cell division, proliferation, and the inhibition of apoptosis. Despite these oncogenic effects, JNK-1 proteins have demonstrated the ability to suppress tumors, as observed in skin cancer and oral cancer contexts [13–15]. The overexpression of JNK-1 has been detected in various cancers, including breast cancer, prostate cancer, liver cancer, among others [16–18].

Throughout history, natural products, better known as secondary metabolites, have played a critical role in the process of drug discovery. These compounds contain pharmacologically active ingredients, leading to the derivation of many drugs and their derivatives from natural sources. Recently, natural products hold significant importance in cancer treatment due to their advantageous properties, including low side effects, cost-effectiveness, potency, and specificity [19–22].
Since the early seventieth, computational modeling withstood as a revolutionary strategy in multiple disciplines of the medical sciences [23–25]. For instance, *In silico* modeling can used in medical imaging besides its use in the drug discovery [26].The emergence of high throughput screening (HTS) and advanced machinery towards the end of the last century shifted research focus towards the exploration of natural products [27,28]. The strategic utilization of isolated natural products as scaffolds for screening libraries has emerged as a distinct approach in modern drug discovery, facilitating the exploration of new leads [29].
Computer-aided drug design (CADD) represents a significant advancement in the field of drug discovery, aiming to minimize errors inherent in traditional methods while reducing costs and time. Two primary approaches within CADD programs are Structural-Based Drug Design (SBDD) and Ligand-Based Drug Design (LBDD) [30–34]. The application of computational methods accelerates the pace of drug discovery and development. Numerous studies have explored computational applications to identify inhibitors for the JNK1 protein, targeting various diseases. For instance, targeting the JNK1 protein in type 2 diabetes has emerged as a crucial objective [35,36]. In the study between your hands, we aimed to investigate the renowned supernatural 3.0 database through extensive multi-stage computational process (E-pharmacophore modeling, molecular docking, MM-GBSA binding free energy calculations, and molecular dynamics simulation) for the intentto discover new anticancer compounds with sufficient proves of their potential JNK1 inhibitory activity.

2. Methods

All computational studies were performed using Maestro v 12.8 by Schrödinger and academic Desmond v6.5 by D.E. Shaw Research for MD.

2.1. Protein preparation

The 3D crystal structure of the JNK1 protein was acquired from the Protein Data Bank (PDB) utilizing the accession code4AWI which specifically encodes for Human JNK1 alpha kinases bound with 4-phenyl-7-azaindoles[37]. To ensure structural integrity and optimal energetics, we employed the Protein Preparation Wizard developed by Schrödinger. This tool facilitated the optimization and refinement of the protein by assigning bond orders, converting selenomethionines into methionines, removing water molecules beyond a 5 Å radius, filling in missing loops using Prime, and optimizing hydrogen bond assignments using PROPKA at a pH of 7.4. Further refinement involved the deletion of water molecules and subsequent minimization using the OPLS4 force field. These steps were crucial for confirming the optimal structural conformation of the protein, thereby ensuring its suitability for subsequent accurate analyses [38–40].

2.2. Ligand preparation and grid generation of receptor protein

For ligand gathering and preparation, we obtained the molecular library from the opened-accessSuper-Natural 3.0 (SN3) databases. Subsequently, energy minimization and ligands optimization were performed using the Macromodel tool of Maestro applying the energy parameters of the OPLS4 force field.

On the other context, the receptor gride generator tab in Glide module was recruited to create orthogonal cubic gride for ligand binding site Inspired by the coordinates of JNK-1, 4AWI, co-crystalized inhibitor. This step is crucial and it inevitably affects the reliability of molecular docking and the accurate representation of protein-ligand interactions [41].

2.3. E-pharmacophore generation and screening

Pharmacophore modeling involves the creation of a model by screening the target structure or ligands, identifying the essential key features for binding and activity. These features include hydrogen bond donors, acceptors, hydrophilic and hydrophobic residues. The generated model afterward can be utilized to screen a library of molecules in search for potential leads that with the desirable pharmacophoric features against the targeted proteins [42,43]. In this study, the PHASE module from Schrödinger was employed for pharmacophore modeling [44].

The E-pharmacophore method was utilized to generate a model using protein-ligand complexes as input. This step yielded a pharmacophore hypothesis that highlights the essential structural features for effective JNK-1 binding (hydrogen bond donors, acceptors, hydrophobic groups, aromatic rings, hydrophilic groups, and ionizable groups). Furthermore, the total energy within the complex is calculated based on the contributions of all pharmacophoric sites and surrounding atoms [45,46].

Subsequently, screening of the Super-Natural 3.0 (SN3) databases on the light of the generated hypothesis was conducted using Phase pharmacophore-based screening to identify the potential inhibitors of JNK1[47].

2.4. Molecular docking and MM-GBSA calculations

For molecular docking analysis, we utilized the Glide software developed by Schrödinger [41]. This tool employs Monte Carlo simulates annealing searching algorithms to sample the possible protein-ligand conformations, and utilizes docking score, a modified ChemScore, to evaluate these conformations. Additionally, Glide applies different levels of penalties it presents to highly accurate estimations. Glide renders the docking process in three integrated modes, High Throughput Virtual Screening (HTVS), which is characterized by its speed and enables the initial identification of ligands for further screening with minimum applied penalties. Conversely, Standard precision (SP) and Extra Precision (XP), exploit more sophisticated scoring functions and higher degree of penalties[48,49].

In this study, the molecules that fit the anticipated pharmacophore hypotheses were subjected to comprehensive docking analysis to validate the pharmacophore hypothesis and capture more accurate affinity predictions.Prior its execution, the docking procedure has been validated through the calculation of RMSD values for the reference ligand before and after docking. HTVS was applied to gather clues about the most potential hits and therefore narrow the examined molecular set. For further refinement, the best 10% in terms of docking score were subsequently subjected to SP analysis. Eventually,XP docking was executed for the compounds that projected the best docking.

Molecular MechanicsGeneralized Born Surface Area (MM/GBSA) calculations provide more coherent binding free energy predictions. Prime module of Schrödinger inputs of three energy values; the energy of the apo protein, the energy of the unbound ligand, and the energy of the protein-ligand complex, to calculate the free binding energy of the system barrowing the energetics of OPLS forcefield. Uniquely, Prime MM-GBSA tool adopts VSGB2.0 as solvent model and applies strict solvation penalties which is known to be significant for both the accuracy and precision of the results.
In this work, we established MM-GBSA calculations for the compounds that disclosed promising docking result in XP docking step to comprehend their JNK-1 binding potential quantitatively as well as qualitatively and to incorporate a high degree of certainty in the conclusions of our docking process [50,51].

2.5. Molecular dynamics simulations

MD investigates the stability of protein-ligand interactions and studiesthe conformational changes and intermolecular forces involved in the protein and ligand contacts through the concepts of molecular mechanics and Newtonian equations of motion. Surprisingly, MD surpasses the other computational analysis in accuracy since it counts the dimension of time and the effects of the physiological environment.MD analysis trajectories hold massive information about the inclinations of the protein and ligand throughout the interaction time. RMSD portrays the dislocations of the protein alpha carbon during the complexation process. Meanwhile, RMSF postulates the fluctuations of each residue in the protein backbone. In this article, MD simulations were carried out using the academic version of Desmond software [52].

The system was firstly enclosed in a box with uniform dimensions of 10 Å to ensure consistency. To reproduce the physiological medium, TIP3P water model and neutralizing charges with sodium and chloride ions were employed [53]. Moreover, Limited-memory Broyden-Fletcher-Goldfarb-Shanno (LBFGS) algorithm was exploited to address the steric clashes in the protein-ligand complex.

The NPT ensemble has been utilized to achieve a temperature of 300 K and a pressure of 1 bar throughout the simulation duration. Eventually, the system underwent an energy minimization process until reaching stability. To manage long-range electrostatic interactions, the Smooth Particle Mesh Ewald (SPME) technique was employed with a tolerance set to 1e-09. Short-range electrostatic interactions were managed using a cutoff radius of 9 Å [54][55].

2.6. ADMETprediction

*In silico*pharmacokinetics and toxicity prediction has gained accountable credibility in the last decades due to its minimal computational cost together with its highly accurate predictions[56].
In this study, the drug like propriety for the selected molecules was calculated using QikProp module In Maestro software package. This tool searches for the presence of particular chemical groups which their presence has pharmacokinetic and/or toxicological repercussions[56].

Accordingly, the compounds have been examined for the alignment with Lipinski's rule of five through the analysis of their corresponding molecular wight, octanol/water partition coefficient, and number of hydrogen bond donors and acceptors.
ProTox-II webserver utilizes molecular similarity, pharmacophores, fragment propensities and machine-learning models to provide a meticulous estimation of various toxicity endpoints, such as acute toxicity, hepatotoxicity, cytotoxicity, carcinogenicity, mutagenicity, immunotoxicity, adverse outcomes pathways and toxicity targets. In this study, we have subjected the molecules that shown the greatest potential in the computational analysis to the ProTox-II webserver to portray their predictable toxicity profile[57][58].

3. Results

In this research, we adopt a comprehensive computational approach to identify potential natural compounds as inhibitors of JNK1 (**Figure 1**).

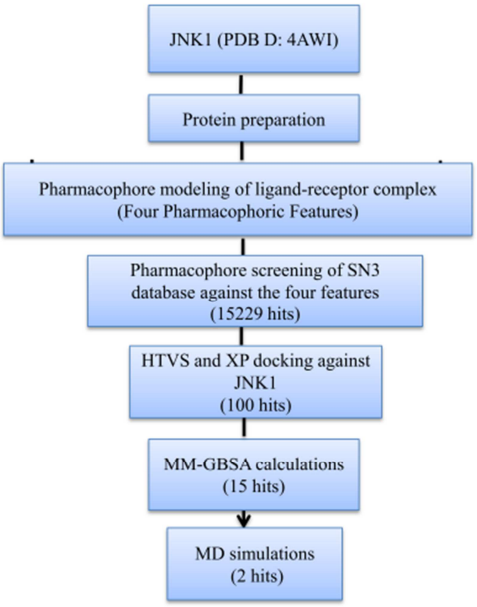

Figure 1: The study workflow.

3.1 E-pharmacophore modeling and screening

We employed receptor-based pharmacophore modeling to derive a pharmacophoric hypothesis from the co-crystallized ligand bound to JNK1 (PDB ID: 4AWI). The generated pharmacophore hypothesis comprised four features, including two aromatic rings (R) and two hydrogen donors (D), as illustrated in **Figure 2**.

A total of 449,008 natural compounds sourced from the SN3 database were subjected to screening against the four features of the pharmacophore hypothesis. This screening process yielded 15,229 compounds that matched all chemical features of the hypothesis.

Subsequently, to explore the interaction of the screened SN3 natural compounds based on the pharmacophore hypothesis, molecular docking was conducted using Glide docking tiers against JNK1, as elaborated in the following section.

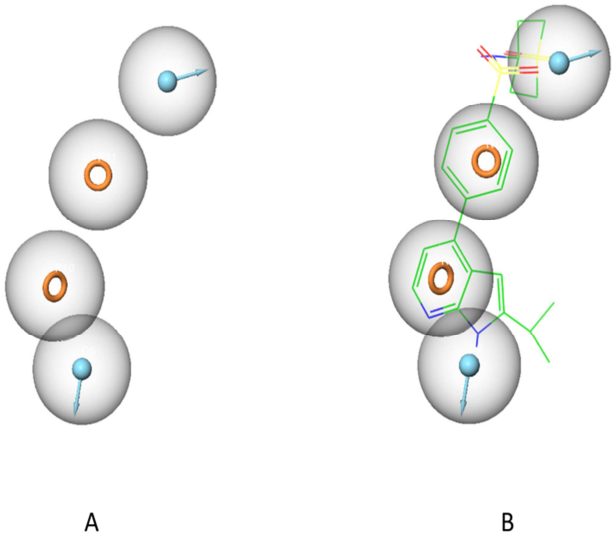

Figure 2: The pharmacophore hypothesis developed using the co-crystalized ligand with JNK1 (PDB D: 4AWI). The hypothesis was generated using "Generate hypothesis from multiple ligands" option of Phase software. Yellow open circle, aromatic ring (R); blue sphere with arrow, hydrogen-bond donor (D). **A.** The pharmacophore hypothesis **B.** The hypothesis aligned with bound ligand.

3.2. Molecular docking and MM-GBSA calculations

Molecular docking was used to dock the natural compounds obtained from the pharmacophore screening against JNK1 binding site. The root mean square deviation (RMSD) between the co-crystallized reference and the re-docked reference is 0.43 Å.

The Phase screen results underwent two rounds of molecular docking against JNK1 using Schrodinger's Glide tool. The compounds underwent filtration via two Glide docking modes, namely High Throughput Virtual Screening (HTVS) and Extra Precision (XP). Initially, molecular docking was conducted to virtually screen a library of 15,229 natural products from the SN3 database using the HTVS docking mode of Glide. Subsequently, the top 100 compounds from HTVS docking were subjected to XP docking mode. This led to the identification of 15 compounds with docking scores ranging from -13.469 to -12.888 kcal/mol, surpassing the binding affinity of the bound ligand (-12.851 kcal/mol) (**Table 1**).

Table 1: Docking scores and MM-GBSA binding energy of the top 15 natural compounds and the reference ligand bound to the JNK1 binding cavity (PDB D: 4AWI).

Compound ID	Docking Score (kcal/mol)	MMGBSA dG Bind (kcal/mol)
SN0239242	**-13.469**	**-69.22**
SN0430786	-13.426	-26.46
SN0334117	-13.413	-41.81
SN0127025	-13.343	-48.6
SN0001583	-13.177	-42.29
SN0422316	-13.14	-50.71
SN0263268	**-13.082**	**-62.58**
SN0200910	-13.068	-46.56
SN0068835	-13.041	-44.82
SN0390869	-12.983	-48.4
SN0010594	-12.963	-33.82
SN0295920	-12.9	-38.32
SN0160811	-12.898	-45.13
SN0046515	-12.897	-35.18
SN0276865	-12.888	-41.38
Bound reference	-12.851	-57.68

Furthermore, the top 15 phytochemicals underwent Molecular Mechanics/Generalized Born Surface Area (MM-GBSA) calculations using Maestro's Prime tool to forecast the free energies of MM-GBSA binding among the three ligand-protein complexes. Compounds SN0239242 and SN0263268 exhibited favorable free binding energies of -69.22 and -62.2 kcal/mol, respectively, when bound with JNK1, while the reference compound displayed a value of -57.68 kcal/mol(**Figure 3**).

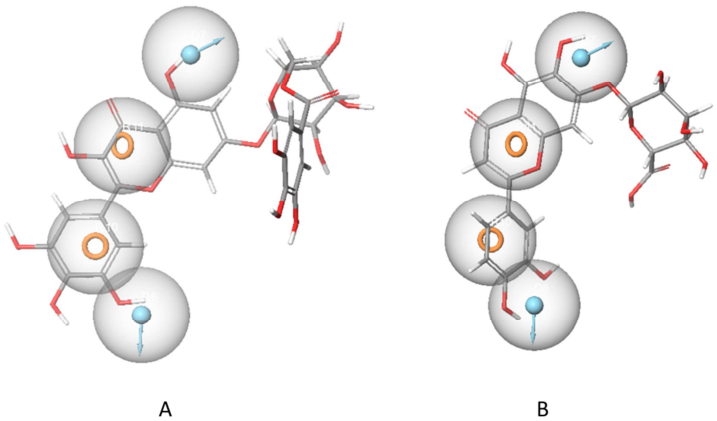

Figure 3: Top two compounds and the reference aligned the pharmacophore hypothesis. **A.** SN0239242 **B.** SN0263268.

Additionally, leveraging the graphical representation of the Schrodinger ligand interaction module, a comprehensive analysis of the molecular interactions between JNK1 and the top two compounds was conducted, as depicted in **Figure 4**.

Additionally, leveraging the graphical representation of the Schrodinger ligand interaction module, a comprehensive analysis of the molecular interactions between JNK1 and the top two compounds was conducted, as depicted in **Figure 4**.

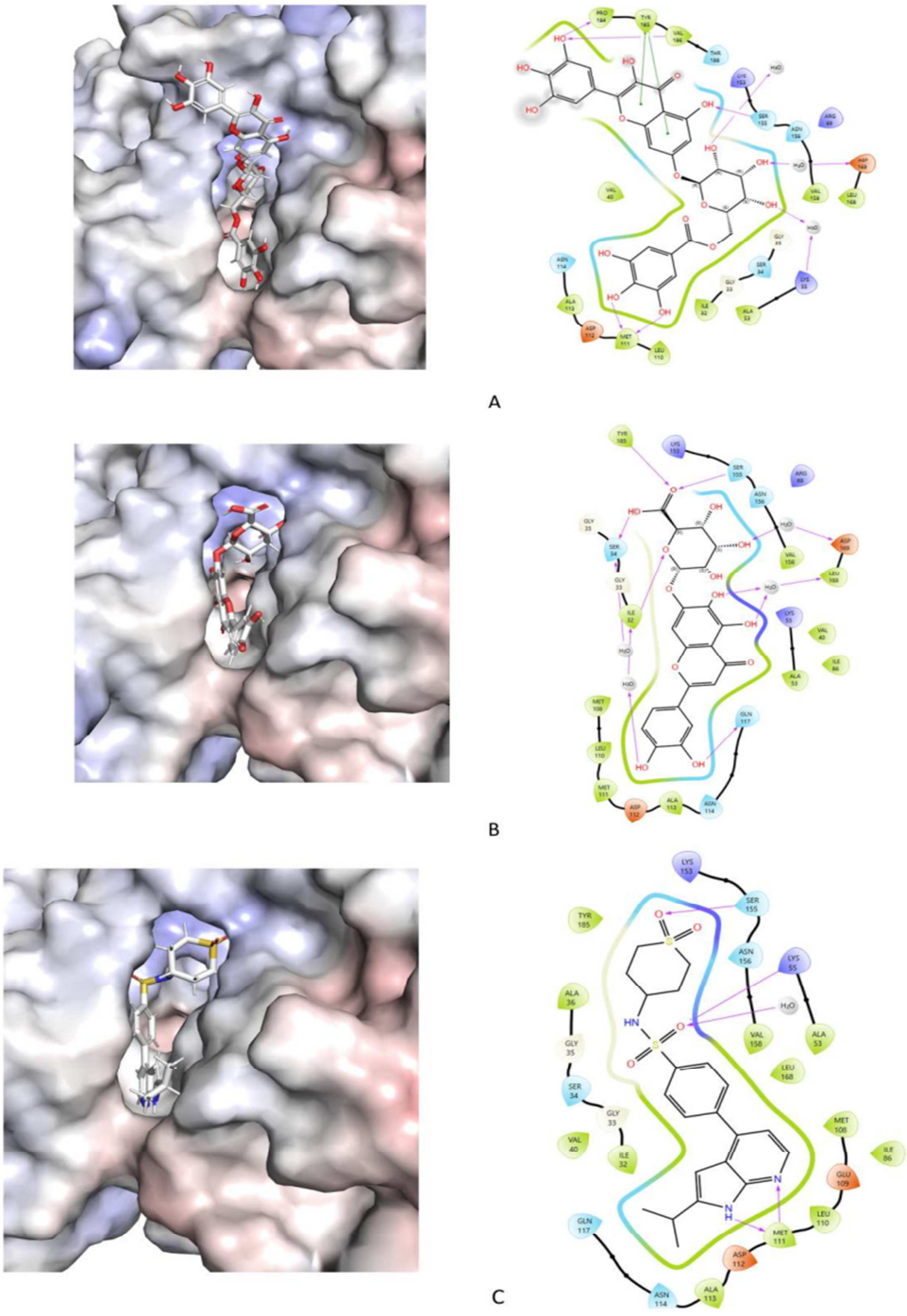

Figure 4:2D and 3D interactions of the top two compounds and the reference with JNK1 (PDB D: 4AWI) using the Glide software. **A.** SN0239242 **B.** SN0263268 **C.** Reference.

SN0239242 formed hydrogen bonds primarily with PRO184 and VAL186. Additionally, SN0239242 engaged in water bridge interactions with LYS55, MET111, and ASP169, further enhancing its binding affinity. SN0263268 demonstrated hydrogen bonding interactions with ILE32, SER34, GLN117, SER155, and TYR185. Moreover, SN0263268 formed water bridge interactions with ILE32, SER34, LEU168, and ASP169, highlighting additional stabilizing interactions within the binding cavity. The reference ligand primarily interacted through hydrogen bonds with LYS55, MET111, and SER155, indicating a comparatively limited interaction profile.

Notably, pi-pi interactions were observed only with TYR185 in the case of SN0239242, suggesting a potential role of aromatic stacking in stabilizing the ligand-protein complex. No pi-pi interactions were observed for SN0263268 or the reference ligand.

3.3. Molecular dynamics

The molecular dynamics (MD) was used forthe top two natural compounds, SN0239242 and SN0263268along with the reference compound for 100 ns.

SN0239242-JNK1 displayed superior stabilization compared to SN0263268-JNK1 and the reference-JNK1, with Root mean square deviation (RMSD) values of 4.41 ± 0.80 Å, 6.13 ± 0.79 Å, and 5.20 ± 0.78 Å, respectively, throughout the simulation period. Despite higher structural fluctuations observed in SN0239242-JNK1 between 30ns and 70ns, the carbon alpha RMSD for the protein remained relatively stable at 2.89 ± 0.35 Å, indicating overall protein stability (**Figure 5**).

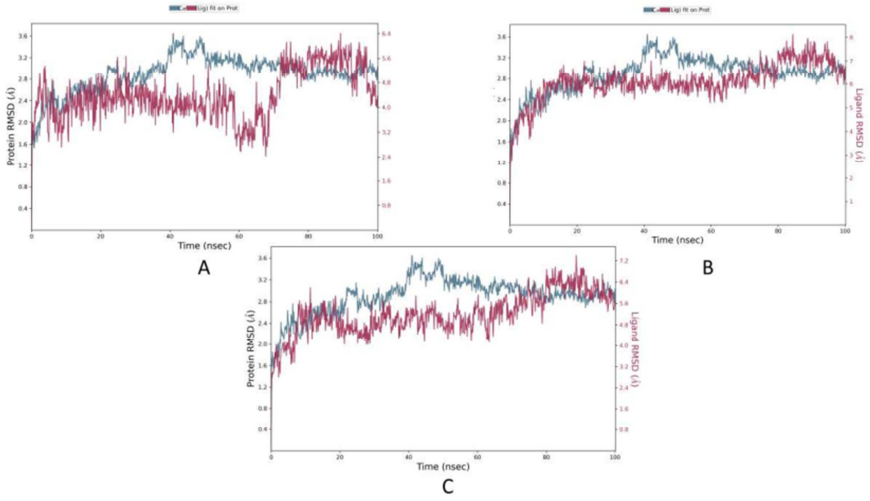

Figure 5: The protein-ligand RMSD plot of the top two compounds and the reference complexed with JNK1 (PDB D: 4AWI) during 100 ns molecular dynamics simulation using Desmond software. **A.** SN0239242 **B.** SN0263268 **C.** Reference.

LEU363 and GLU364 exhibited the highest fluctuations, with Root-mean-square fluctuations (RMSF) values of 4.044 Å and 5.950 Å, respectively, while the remaining protein residues showed lower fluctuations, with an average RMSF of 1.15 ± 0.79 Å (**Figure 6**).

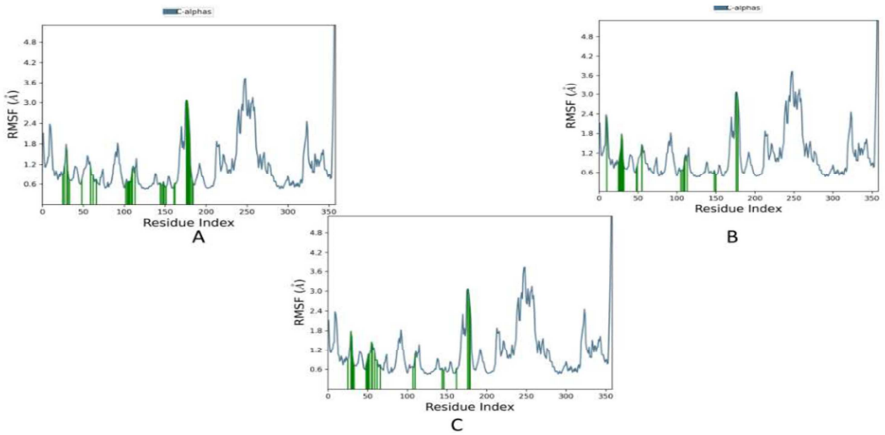

Figure 6: Protein RMSF plot displaying JNK1 (PDB D: 4AWI) bound to the top two compounds and the reference during 100 ns molecular dynamics simulation using Desmond software. **A.** SN0239242 **B.** SN0263268 **C.** Reference.

Ligand Root Mean Square Fluctuation (L-RMSF) analysis highlighted significant changes in ligand atom positions during the simulation period. On average, the RMSF values with respect to the protein-ligand complex for SN0239242-JNK1, SN0263268-JNK1, and reference-JNK1 were 1.93 ± 0.68 Å, 1.64 ± 0.65 Å, and 1.80 ± 0.68843 Å, respectively (**Figure 7**).

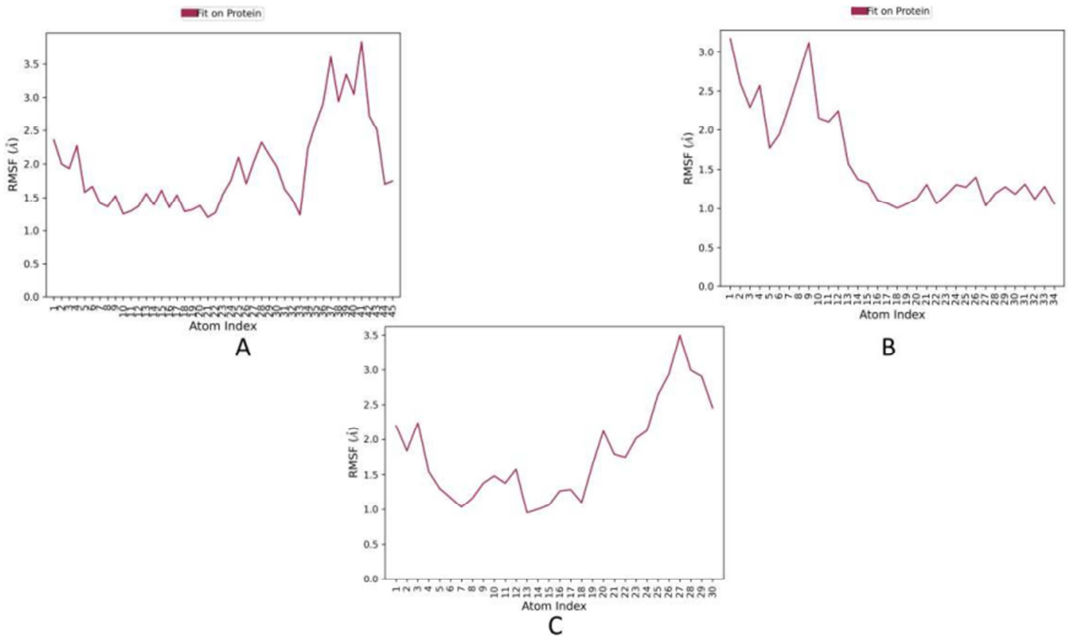

Figure 7: Ligand RMSF plot displaying the top two compounds and the reference with JNK1 (PDB D: 4AWI) during 100 ns molecular dynamics simulation using Desmond software. **A.** SN0239242 **B.** SN0263268 **C.** Reference.

Furthermore, the non-bonded intermolecular interactions between the JNK1 binding residues and the top two natural compounds, as well as the bound reference, observed during the 100 ns MD simulation, are depicted in **Figure 8**.

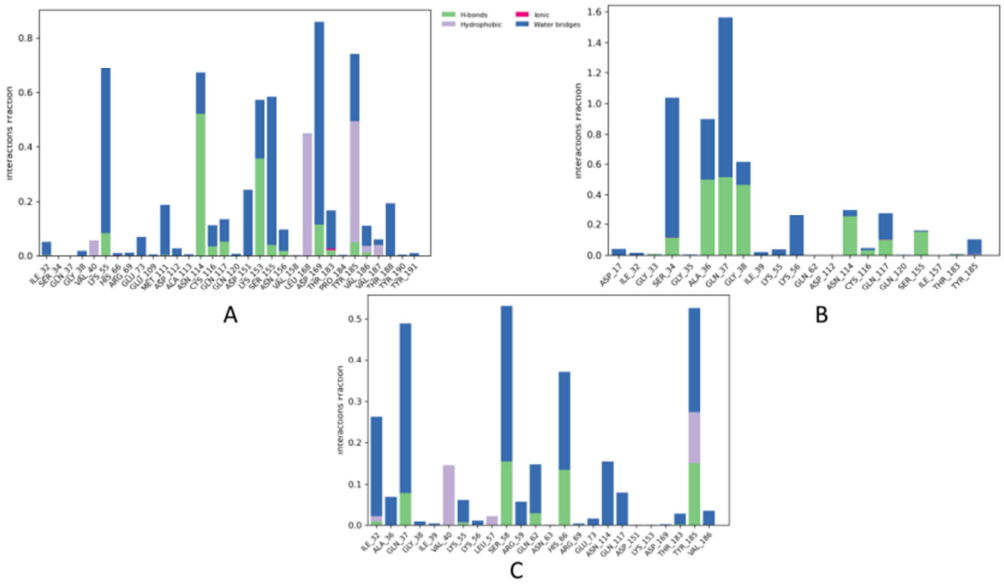

Figure 8: Protein-ligand contact histogram of the top two compounds and the reference complexed with JNK1 (PDB D: 4AWI) during 100 ns molecular dynamics simulation using Desmond software. **A.** SN0239242 **B.** SN0263268 **C.** Reference.

For hydrogen bonds, SN0239242 displayed significant interactions with ASN114 (52%) and LYS153 (36%). Similarly, SN0263268 formed hydrogen bonds with ALA36 (50%), GLN37 (51%), and GLY38 (47%). In contrast, the reference compound exhibited weaker hydrogen bonding interactions with SER58 (16%), HIS66 (14%), and TYR185.(%15)
Furthermore, analysis of water bridges revealed distinct patterns of interaction. SN0239242 formed water bridges predominantly with LYS55 (61%), SER155 (55%), and ASP169 (75%). SN0263268 engaged in water bridge interactions with SER34 (92%), ALA36 (40%), and GLN37 (101%). The reference compound showed fewer water bridge interactions, with notable participation from ILE32 (24%), GLN37 (41%), and TYR185.(%25)
Regarding hydrophobic interactions, SN0239242 demonstrated notable interactions with LEU168 (45%) and TYR185 (45%). However, SN0263268 did not exhibit significant hydrophobic interactions in this context. The reference compound showed limited hydrophobic interactions, primarily with VAL40 (15%) and TYR185 (12%).

3.4. ADMET prediction

The best scoring molecules were subjected to a comprehensive ADMET analysis using QikProb tool and Pro Tox II webserver. Beyond this, we harnessed QikProb to examine the compliance of the molecules with Lipinski's rule of five through the prediction of molecular weight in KDa,hydrogen bond donors (HBD) and acceptors (HBA), and octanol/H2O partition coefficient (QPlogPo/w). Furthermore, two cell membrane penetration factors were estimated including bloodbrain barrier permeability (QPlogBB) and cell membrane permeability (QPPCaco-2) in nm/sec considering Caco-2 cells as model for the gut-blood barrieras summarized in Table 2.

Table 2: The predicted ADMET descriptors for SN0263268 and SN0239242 *via*QikProb tool of Maestro

Title	mol MW	HBD	HBA	QPlogPo/w	QPPCaco-2	QPlogBB	RuleOfFive
SN0263268	478.365	6	13.05	-0.952	0.133	-4.748	2
SN0239242	632.487	10	17.05	-2.249	0.032	-7.444	3
Reference value	130-725	≤6	2-20	-2 - 6.5	<25 poor; >500 great	-3 – 1.2	0 - 4

The Pro Tox II webserver displayed the toxicological profile of the two compounds in three aspects; oral toxicity, organ toxicities, and toxicities end points. Oral toxicity was symbolized in median lethal dose (LD50) calculated in milligram per kilogram of body weight. Meanwhile, organ toxicities anticipated the toxicity risk against the vital organs,cardiotoxicity, hepatotoxicity, neurotoxicity, and nephrotoxicity. Eventually, the major toxicity endpoints were predicted which encompassed carcinogenicity, immunotoxicity, mutagenicity, and cytotoxicity (Table 3).

Table 3: The predicted oral toxicity, organ toxicities, and toxicities end points *via* Pro Tox II webserver.

		SN0263268	SN0239242
Oral Toxicity	Toxicity Class	5	5
	LD50 (mg/kg)	5000	5000
Organ toxicity	Hepatotoxicity	Inactive	Inactive
	Neurotoxicity	Inactive	Inactive
	Nephrotoxicity	Active	Active
	Cardiotoxicity	Inactive	Inactive
	Carcinogenicity	Active	Inactive
	Immunotoxicity	Inactive	Inactive
	Mutagenicity	Inactive	Inactive
	Cytotoxicity	Inactive	Inactive

4. Discussion

The study explores the role of human JNK1 genes, which are often overexpressed in various cancers including skin, liver, breast, brain tumors, leukemia, multiple myeloma, and lymphoma. Computational methods have become indispensable in drug discovery, spanning from target identification to lead optimization[25,59]. A primary objective in this field is the identification of novel chemical entities capable of binding to target proteins to induce the desired biological response. A receptor-based pharmacophore modeling was used to build a pharmacophoric hypothesis from the co-crystallized ligand bound to JNK1. The obtained pharmacophore hypothesis consisted of four features (aromatic rings (R) and two hydrogen donors (D)). A library of natural compounds from the SN3 database was screened against the four features of the pharmacophore hypothesis resulting in 15,229 compounds that matched all chemical features of the hypothesis. Then, molecular docking, MM-GBSA calculations and molecular dynamics were usedto validate this pharmacophoric studies, as elaborated in the following section.
Molecular docking, a pivotal technique in structure-based drug design, was utilized to probe the binding interactions and affinities of ligands within the JNK1 binding site [39–41][60]. The root mean square deviation (RMSD) between the co-crystallized reference and the re-docked reference, measuring at 0.43 Å, underscores the precision of the docking methodology employed in this investigation. The compounds obtained from the pharmacophore screening were docked against JNK1 binding cavity using two Glide docking modes (High Throughput Virtual Screening (HTVS) and Extra Precision (XP)). HTVS mode facilitates rapid screening by minimizing intermediate conformations and employing final torsion refinement and sampling. Subsequently, the top compounds from HTVS docking were subjected to XP docking mode, renowned for its extensive sampling and intricate scoring

function that eliminates false positives. Additionally, XP penalizes compounds with reduced complementarity with the target active site. This led to the discovery of 15 natural compounds with docking scores surpassing the binding affinity of the bound ligand. These compounds were subjected to Molecular Mechanics/Generalized Born Surface Area (MM-GBSA) calculations using Maestro's Prime tool to predict the free energies of MM-GBSA binding among the three ligand-protein complexes. MM-GBSA calculation accounts for the solvent effect on ligand binding to the target. Compounds SN0239242 and SN0263268 exhibited favorable free binding energies compared to the reference compound. Notably, the top two ligands conform to the four pharmacophore features. The analysis of the interactions between the top two compounds and the reference ligand with the JNK1 binding cavity revealed distinct binding patterns. Overall, the favorable docking scores and MM-GBSA binding energies of SN0239242 and SN0263268, along with their specific interactions within the JNK1 binding cavity, indicate their repressive potential.

The molecular dynamics (MD) simulation analysis provided valuable insights into the molecular interactions within the protein-ligand complex, assessing their stability under simulated physiological conditions using the Maestro Desmond module. The MD simulation focused on the top two natural compounds, SN0239242 and SN0263268, which exhibited stronger ligand-protein interactions, along with the reference compound identified through XP Glide docking. Root mean square deviation (RMSD), measured with respect to the initial structure, indicated notable differences in stability among the complexes. Root-mean-square fluctuations (RMSF) analysis provided insights into the fluctuations of individual protein residues over time. Higher peaks in RMSF graphs correspond to residues experiencing greater fluctuations. The protein showed low RMSF values confirming the protein stability. Furthermore, the non-bonded intermolecular interactions between the JNK1 binding residues and the top two natural compounds, as well as the bound reference. Many of the ligand-protein interactions observed during the docking study were consistently observed throughout the MD simulation. Interestingly, the tested compounds explicit numerous JNK-inhibitors explosive interactions. A series of 4-quinolone JNK inhibitors discovered by Roche interact with the hinge region`sMet111 and Ile32[61]. Moreover, it has been reported that interactions with Glu109, Leu110, met111, Gln37, Lys55 endorse the selectivity of JNK inhibitors over CDK and P38 inhibition as in Aminopyridines[62]. Furthermore, a novel class of 2-aminopyridopyrimidinone-based JNK inhibitors reported by Zheng et al occupies the ATP binding site and interact with Lys55[63]. Abbott reported that 4-anilinopyrimidines JNK1 inhibitors stick to JNK1 binding site through crucial hydrogen bond with Met111[64]. Recalling the interaction patterns for SN0239242 and SN0263268, these studies confirm the JNK1 inhibitory, hence the antitumor potential of these compounds.

The pharmacokinetic and toxicity profile comprises essential parameters that abort significant number of the discovered medication before they reach the clinical utility. Depending on this concept, the early anticipation of ADMET profile saves tremendous effort in the journey of drug discovery and development[58].It can be seen from table 2 that these compounds hold interesting drug likability traits nevertheless, they violate Lipinski's rule of five in multiple terms[65]. SN0263268 has shown two violations since it outnumbered the stated HB donor and acceptors, otherwise, its predicted partition coefficient was acceptable. Conversely, the predicted QPlogPo/w forSN0239242 was slightly lower than the acceptable limit. SN0239242 also breached Lipinski's indicated numbers of HB donors and acceptors. QPPCaco-2 and QPlogBBindicated poor gut and BBB penetration for both molecules. Regarding the summarized Pro-Tox toxicity reports in Table 3, both compounds carried no risk of oral toxicity as it can be observed in their corresponding toxicity classes and LD50 data. organ toxicity parameters suggested possible nephrotoxicity risk with the tested molecules, however, there was no reported cardiac, hepatic, or neurotoxicities. Pro-Tox predicted no toxicity endpoints for SN0239242. SN0263268 on the other hand postulated carcinogenic possibility, nonetheless, no detected risk of immunotoxicity, mutagenicity, or cytotoxicity.

5. Conclusion

The human JNK1 protein kinase plays a crucial role in various signal transduction pathways, particularly in the MAPK-signaling pathway. Overexpression of JNK1 is a common feature observed across numerous cancer types. In this study, computational methodologies were employed to identify potential JNK1 inhibitors from natural compounds. Specifically, two phytochemicals, SN0239242 and SN0263268, were pinpointed as promising candidates. These compounds were selected based on their demonstrated ability to interact with JNK1, as revealed through pharmacophore modeling and screening, molecular docking analyses, and their favorable MM-GBSA binding energies. Furthermore, their stability under simulated physiological conditions was confirmed through molecular dynamics simulations. Further experimental validation is warranted to explore their efficacy in combating cancer and potentially contributing to the development of new therapeutic interventions.

Funding

No funding was received for this project.

Acknowledgment

We acknowledge Mme Katia Dekimeche from Schrodinger for the technical support and help.

Conflict of interest

The authors declare no conflict of interest.

Data availability statement

All data required to support this study is already included in the manuscript.

List of abbreviations

CADD: Computer-aided Drug Design
JNK1: Human c-Jun N-terminal kinase 1
MAPKs: Mitogen-activated protein kinases
MM-GBSA: Molecular mechanics with generalized Born and surface area
MD: Molecular Dynamics.
RMSD: Root Mean Square Deviation
RMSF: Root Mean Square Fluctuation
HTVS: High throughput virtual screening
SP: Standard Precision
XP: Extra precision

6. References

1. Johnson GL, Lapadat R. Mitogen-activated protein kinase pathways mediated by ERK, JNK, and p38 protein kinases. Science (80-). 2002;298(5600):1911–2.
2. Kyriakis JM, Avruch J. Mammalian mitogen-activated protein kinase signal transduction pathways activated by stress and inflammation. Physiol Rev. 2001;81(2):807–69.
3. Kyriakis JM, Avruch J. pp54 microtubule-associated protein 2 kinase. A novel serine/threonine protein kinase regulated by phosphorylation and stimulated by poly-L-lysine. J Biol Chem. 1990 Oct;265(28):17355–63.
4. Bogoyevitch MA, Kobe B. Uses for JNK: the many and varied substrates of the c-Jun N-terminal kinases. Microbiol Mol Biol Rev. 2006 Dec;70(4):1061–95.
5. Hibi M, Lin A, Smeal T, Minden A, Karin M. Identification of an oncoproteinand UV-responsive protein kinase that binds and potentiates the c-Jun activation domain. Genes Dev. 1993;7(11):2135–48.
6. Gupta S, Barrett T, Whitmarsh AJ, Cavanagh J, Sluss HK, Dérijard B, et al. Selective interaction of JNK protein kinase isoforms with transcription factors. EMBO J. 1996 Jun;15(11):2760–70.
7. Kyriakis JM, Banerjee P, Nikolakaki E, Dai T, Rubie EA, Ahmad MF, et al. The stress-activated protein kinase subfamily of c-Jun kinases. Nature. 1994 May;369(6476):156–60.
8. Chen F. JNK-induced apoptosis, compensatory growth, and cancer stem cells. Cancer Res. 2012 Jan;72(2):379–86.
9. Minden A, Karin M. Regulation and function of the JNK subgroup of MAP kinases. Biochim Biophys Acta - Rev Cancer. 1997;1333(2).
10. Sabapathy K, Jochum W, Hochedlinger K, Chang L, Karin M, Wagner EF. Defective neural tube morphogenesis and altered apoptosis in the absence of both JNK1 and JNK2. Mech Dev. 1999;89(1–2):115–24.
11. Johnson GL, Nakamura K. The c-jun kinase/stress-activated pathway: Regulation, function and role in human disease. Biochim Biophys Acta - Mol Cell Res. 2007;1773(8):1341–8.
12. Dhillon AS, Hagan S, Rath O, Kolch W. MAP kinase signalling pathways in cancer. Oncogene. 2007 May;26(22):3279–90.
13. Dérijard B, Hibi M, Wu IH, Barrett T, Su B, Deng T, et al. JNK1: A protein kinase stimulated by UV light and Ha-Ras that binds and phosphorylates the c-Jun activation domain. Cell. 1994;76(6):1025–37.
14. Ahlemann M, Zeidler R, Lang S, Mack B, Gires O, Mu M. Overexpression Facilitates mTOR-dependent Growth Transformation. Mol Carcinog. 2006;967(May):957–67.
15. Gkouveris I, Nikitakis NG. Role of JNK signaling in oral cancer: A mini review. Tumor Biol. 2017;39(6).
16. Sivaraman VS, Wang H, Nuovo GJ, Malbon CC. Hyperexpression of mitogen-activated protein kinase in human breast cancer. J Clin Invest. 1997 Apr;99(7):1478–83.
17. Parra E. Inhibition of JNK-1 by small interfering RNA induces apoptotic signaling in PC-3 prostate cancer cells. Int J Mol Med. 2012;30(4):923–30.
18. Chang Q, Zhang Y, Beezhold KJ, Bhatia D, Zhao H, Chen J, et al. Sustained JNK1 activation is associated with altered histone H3 methylations in human liver cancer. J Hepatol. 2009 Feb;50(2):323–33.
19. Majolo F, de Oliveira Becker Delwing LK, Marmitt DJ, Bustamante-Filho IC, Goettert MI. Medicinal plants and bioactive natural compounds for cancer treatment: Important advances for drug discovery. Phytochem Lett. 2019;31:196–207.
20. Mishra BB, Tiwari VK. Natural products: An evolving role in future drug discovery. Eur J Med Chem. 2011;46(10):4769–807.
21. Tran AT, Watson EE, Pujari V, Conroy T, Dowman LJ, Giltrap AM, et al. Sansanmycin natural product analogues as potent and selective anti-mycobacterials that inhibit lipid i biosynthesis. Nat Commun. 2017;8:1–9.
22. Rajesh E, Sankari LS, Malathi L, Krupaa JR. Naturally occurring products in cancer therapy. J Pharm Bioallied Sci. 2015 Apr;7(Suppl 1):S181-3.
23. Challan SB, Khater SI, Rashad AM. Preparation, molecular modeling and in-vivo evaluation of 99mTc-Oseltamivir as a tumor diagnostic agent. Int J Radiat Res. 2022;20(3):635–42.
24. Sanad MH, Sakr TM, Abdel-Hamid WHA, Marzook EA. In silico study and biological evaluation of 99mTc-tricabonyl oxiracetam as a selective imaging probe for AMPA receptors. J Radioanal Nucl Chem. 2017;314(3):1505–15.
25. Yu W, MacKerell AD. Computer-Aided Drug Design Methods. In 2017. p. 85–106. Available from: http://link.springer.com/10.1007/978-1-4939-6634-9_5
26. Sanad MH, Farag AB, Bassem SA, Marzook FA. Radioiodination of zearalenone and determination of *Lactobacillus plantarum* effect of on zearalenone organ distribution: In silico study and preclinical evaluation. Toxicol Reports. 2022;9:470–479.

27. Newman DJ, Cragg GM. Natural Products As Sources of New Drugs over the 30 Years from 1981 to 2010. J Nat Prod. 2012 Mar;75(3):311–35.
28. Wolfender BDJ luc, Dias DA. The pharmaceutical industry and natural products : historical status and new trends. 2014;
29. Barnes EC, Kumar R, Davis RA. The use of isolated natural products as scaffolds for the generation of chemically diverse screening libraries for drug discovery. Nat Prod Rep. 2016;33(3):372–81.
30. Hung C lun, Chen C chun. Computational Approaches for Drug Discovery. 2014;418:412–8.
31. Martin L, Hutchens M, Hawkins C. Trial watch: Clinical trial cycle times continue to increase despite industry efforts. Nat Rev Drug Discov. 2017 Mar;16(3):157.
32. Simoens S, Huys I. R&D Costs of New Medicines: A Landscape Analysis. Front Med. 2021;8(October):1–6.
33. Macalino SJY, Gosu V, Hong S, Choi S. Role of computer-aided drug design in modern drug discovery. Arch Pharm Res. 2015;38(9):1686–701.
34. Shaker B, Ahmad S, Lee J, Jung C, Na D. In silico methods and tools for drug discovery. Comput Biol Med. 2021;137(September):104851.
35. Yang R, Zhao G, Yan B. Discovery of Novel c-Jun N-Terminal Kinase 1 Inhibitors from Natural Products: Integrating Artificial Intelligence with Structure-Based Virtual Screening and Biological Evaluation. Molecules. 2022;27(19).
36. Han S young. c-Jun N-Terminal Kinase Signaling Inhibitors Under Development. 2008;24(2):93–100.
37. Saur IML, Panstruga R, Schulze-Lefert P. NOD-like receptor-mediated plant immunity: from structure to cell death. Nat Rev Immunol. 2021;21(5):305–18.
38. Liddle J, Bamborough P, Barker MD, Campos S, Chung CW, Cousins RPC, et al. 4-Phenyl-7-azaindoles as potent, selective and bioavailable IKK2 inhibitors demonstrating good in vivo efficacy. Bioorganic Med Chem Lett. 2012;22(16):5222–6.
39. Madhavi Sastry G, Adzhigirey M, Day T, Annabhimoju R, Sherman W. Protein and ligand preparation: parameters, protocols, and influence on virtual screening enrichments. J Comput Aided Mol Des. 2013 Mar;27(3):221–34.
40. De Vita S, Lauro G, Ruggiero D, Terracciano S, Riccio R, Bifulco G. Protein Preparation Automatic Protocol for High-Throughput Inverse Virtual Screening: Accelerating the Target Identification by Computational Methods. J Chem Inf Model. 2019;59(11):4678–90.
41. Halgren TA, Murphy RB, Friesner RA, Beard HS, Frye LL, Pollard WT, et al. Glide: A New Approach for Rapid, Accurate Docking and Scoring. 2. Enrichment Factors in Database Screening. J Med Chem. 2004;47(7):1750–9.
42. Giordano D, Biancaniello C, Argenio MA, Facchiano A. Drug Design by Pharmacophore and Virtual Screening Approach. Pharmaceuticals. 2022;15(646):1–16.
43. Rella M, Rushworth CA, Guy JL, Turner AJ, Langer T, Jackson RM. Structure-based pharmacophore design and virtual screening for novel angiotensin converting enzyme 2 inhibitors. J Chem Inf Model. 2006;46(2):708–16.
44. Salam NK, Nuti R, Sherman W. Novel method for generating structure-based pharmacophores using energetic analysis. J Chem Inf Model. 2009 Oct;49(10):2356–68.
45. Dixon SL, Smondyrev AM, Rao SN. PHASE: A novel approach to pharmacophore modeling and 3D database searching. Chem Biol Drug Des. 2006 May;67(5):370–2.
46. Venkatesan A, Rambabu M, Jayanthi S, Febin Prabhu Dass J. Pharmacophore feature prediction and molecular docking approach to identify novel anti-HCV protease inhibitors. J Cell Biochem. 2018 Jan;119(1):960–6.
47. Patel P, Singh A, Patel VK, Jain DK, Veerasamy R, Rajak H. Pharmacophore Based 3D-QSAR, Virtual Screening and Docking Studies on Novel Series of HDAC Inhibitors with Thiophen Linker as Anticancer Agents. Comb Chem High Throughput Screen. 2016;19(9):735–51.
48. Friesner RA, Banks JL, Murphy RB, Halgren TA, Klicic JJ, Mainz DT, et al. Glide: A New Approach for Rapid, Accurate Docking and Scoring. 1. Method and Assessment of Docking Accuracy. J Med Chem. 2004;47(7):1739–49.
49. Thangaraju P, Narasimhan G, Ramamurthy VA, Gurunthalingam MP, Yella SST, Venkatesan S, et al. Molecular Docking Analysis of Adhatoda vasica with Thromboxane A(2) Receptor (TXA(2)R) (6IIU) and Antiviral Molecules for Possible Dengue Complications. Infect Disord Drug Targets. 2023;23(1):e180722206836.
50. Elbadwi FA, Khairy EA, Alsamani FO, Mahadi MA, Abdalrahman SE, Alsharf Z, et al. Identification of novel transmembrane Protease Serine Type 2 drug candidates for COVID-19 using computational studies. Informatics Med Unlocked. 2021;26:100725.
51. Alzain A, Elbadwi F, Alsamani F. Discovery of novel TMPRSS2 inhibitors for COVID-19 using in silico fragment-based drug design, molecular docking, molecular dynamics, and quantum mechanics studies. Informatics Med Unlocked. 2022 Feb;29:100870.
52. Hollingsworth SA, Dror RO. Molecular Dynamics Simulation for All. Neuron. 2018 Sep;99(6):1129–43.
53. Ash J, Fourches D. Characterizing the Chemical Space of ERK2 Kinase Inhibitors Using Descriptors Computed from Molecular Dynamics Trajectories. J Chem Inf Model. 2017;57(6):1286–99.
54. Yu Y, Zhang G, Han T, Liu H, Huang H. Potential Material Basis of Yupingfeng Powder for the Prevention and Treatment of 2019 Novel Coronavirus Pneumonia: A Study Involving Molecular Docking and Molecular Dynamic Simulation Technology. Biomed Res Int. 2022;2022:7892397.
55. Alam P, Tyagi R, Farah MA, Rehman MT, Hussain A, AlAjmi MF, et al. Cytotoxicity and molecular docking analysis of racemolactone I, a new sesquiterpene lactone isolated from Inula racemosa. Pharm Biol. 2021 Dec;59(1):941–52.
56. Ferreira LLG, Andricopulo AD. ADMET modeling approaches in drug discovery. Drug Discov Today. 2019;24(5):1157–65.

57. Banerjee P, Eckert AO, Schrey AK, Preissner R. ProTox-II: A webserver for the prediction of toxicity of chemicals. Nucleic Acids Res. 2018;46:W257–63.
58. Adelusi TI, Oyedele AQK, Boyenle ID, Ogunlana AT, Adeyemi RO, Ukachi CD, et al. Molecular modeling in drug discovery. Vol. 29, Informatics in Medicine Unlocked. Elsevier Ltd; 2022. p. 100880.
59. Sanad MH, Farag AB, Rizvi SFA. In silico and in vivo study of radio-iodinated nefiracetam as a radiotracer for brain imaging in mice. Radiochim Acta [Internet]. 2021 Jul 27;109(7):575–82.
60. Sanad MH, Rizvi SFA, Farag AB. Radiosynthesis and in silico bioevaluation of 131 I-Sulfasalazine as a highly selective radiotracer for imaging of ulcerative colitis. Chem Biol Drug Des. 2021 Nov 29;98(5):751–61.
61. Gong L, Tan Y chou, Boice G, Abbot S, Mccaleb K, Iyer P, et al. Bioorganic & Medicinal Chemistry Letters Discovery of a novel series of 4-quinolone JNK inhibitors. Bioorg Med Chem Lett. 2012;22(24):7381–7.
62. Thi M, Duong H, Lee J hwa, Ahn H chul. C-Jun N-terminal kinase inhibitors : Structural insight into kinase- inhibitor complexes. Comput Struct Biotechnol J. 2020;18:1440–57.
63. Zheng K, Park CM, Iqbal S, Hernandez P, Park H, Lograsso P V, et al. Pyridopyrimidinone derivatives as potent and selective c-jun N-terminal kinase (JNK) inhibitors. ACS Med Chem Lett. 2015;6(4):413–8.
64. Liu M, Xin Z, Clampit JE, Wang S, Gum RJ, Haasch DL, et al. Synthesis and SAR of 1,9-dihydro-9-hydroxypyrazolo[3,4-b]quinolin-4-ones as novel, selective c-Jun N-terminal kinase inhibitors. Bioorganic Med Chem Lett. 2006;16(10):2590–4.
65. Lipinski CA, Lombardo F, Dominy BW, Feeney PJ. Experimental and computational approaches to estimate solubility and permeability in drug discovery and development settings. 2001;46:3–26.